Neurobiology of Disease, 2008

32 (2), 281-292

Role of caspases, calpain and cdk 5 in ammonia-induced cell death in developing brain cells

Laurène Cagnon and Olivier Braissant

Inborn Errors of Metabolism, Clinical Chemistry Laboratory,

Centre Hospitalier Universitaire Vaudois and University of Lausanne,

Switzerland.

Corresponding author: Dr. Olivier Braissant,

Clinical Chemistry Laboratory, CHUV

CI 02-33, Avenue Pierre Decker 2,

1011 – Lausanne, Switzerland.

E-mail: Olivier.Braissant@chuv.ch

Tel: +41 21 314 41 52; Fax: +41 21 314 35 46.

Abstract

Hyperammonemia in neonates and infants causes irreversible damages in the developing CNS due to brain cell loss. Elucidating the mechanisms triggering ammonia-induced cell death in CNS is necessary for the development of neuroprotective strategies. We used reaggregated developing brain cell cultures derived from fetal rat telencephalon exposed to ammonia as an experimental model. Ammonia induced neuronal and oligodendroglial death, triggered apoptosis and activated caspases and calpain. Probably due to calpain activation, ammonia caused the cleavage of the cyclin-dependent kinase 5 activator, p35, to p25, the cdk5/p25 complex being known to lead to neurodegeneration. Roscovitine, a cdk5 inhibitor, protected neurons from ammonia-induced cell death. However, roscovitine also impaired axonal growth, probably through inhibition of the remaining cdk5/p35 activity, which is involved in neurite outgrowth. Thus, cdk5 appears as a promising therapeutic target for treating hyperammonemic newborns and infants, especially if one develops specific cdk5/p25 inhibitors.

Key words

Ammonia, caspase, calpain, cdk5, roscovitine, neuroprotection.

Introduction

Hyperammonemia in neonates and infants is mainly due to defects of the urea cycle enzymes or other inborn errors of metabolism, and causes irreversible damages in the developing CNS such as cortical atrophy, ventricular enlargement, demyelination, and hypodensities of gray and white matter. Irreversible lesions occur in prolonged hyperammonemia and/or high blood ammonia levels (for recent reviews see Cagnon and Braissant, 2007; and Gropman et al. 2007). The recent use of alternative-pathway therapies detoxifying ammonia improved the survival of patients (Enns et al., 2007). However, the improved survival was correlated with a worsened neurological and cognitive outcome. Thus, the development of neuroprotective therapeutics is crucial for the improvement of the neurological outcome of neonates and infants experiencing hyperammonemia.

Ammonia induces cell death in primary cultures of neurons (Klejman et al., 2005), but not of astrocytes (Widmer et al., 2007), if ammonia exposure remains in pathophysiologically relevant concentrations (up to 5 mM). Moreover, we previously showed that ammonia inhibits axonal outgrowth (Braissant et al., 2002). Mechanisms of ammonia cytotoxicity include NMDA excitotoxicity, oxidative stress, cerebral energy deficit, alteration of nitric oxide synthesis, and induction of mitochondrial permeability transition (for a review, see Cagnon and Braissant, 2007). Elucidating the precise molecular mechanisms triggering ammonia-induced brain cell death will allow to identify new therapeutic targets.

Caspases are cysteine proteases playing key roles in apoptosis (Rupinder et al., 2007). Caspases-3 and -9, as well as the dephosphorylation of the pro-apoptotic protein Bad, have been shown to be involved in ammonia-induced apoptosis of hippocampal neurons in primary

cultures (Yang et al., 2003; Yang et al., 2004). Other proteases such as calpain also contribute to apoptosis (McCollum et al., 2002), and calpain activation is involved in various neurological disorders such as ischemia, ethanol neurotoxicity, as well as Alzheimer's and Parkinson's diseases (Mouatt-Prigent et al., 1996; Blomgren et al., 2001; Rajgopal and Vemuri, 2002; Raynaud and Marcilhac, 2006). Moreover, calpain activation is responsible for the cleavage of p35 to p25, which are both activators of the cyclin-dependent kinase 5 (cdk5) (Lee et al., 2000). In neurons, cdk5/p35 promotes survival and neurite outgrowth while cdk5/p25 induces neuronal death through an abnormal activation of cdk5 (O'Hare et al., 2005). It was shown that pharmacological inhibitors of calpain can prevent p35 cleavage and the subsequent neuronal death (Lee et al., 2000).

The aim of the present work was to test whether caspases, calpain, and cdk5/p25 were involved in ammonia-induced death of developing brain cells, and if so, whether inhibiting these death-promoting proteins could protect brain cell survival. For this purpose, we used reaggregated developing brain cell cultures derived from fetal rat telencephalon treated with ammonia as an experimental model for the developing brain exposed to hyperammonemia (Honegger and Monnet-Tschudi, 2001; Braissant et al., 2002; Braissant et al., 2008). We provide evidence that ammonia exposure activates caspases and calpain, the latter causing the cleavage of p35 to p25. Moreover, roscovitine, an inhibitor of cdk5, significantly reduced the ammonia-induced death of developing brain cells but did not prevent ammonia-induced impairment of axonal outgrowth.

Material and Methods

Reagents and antibodies

DMEM powder without sodium pyruvate and sodium bicarbonate was purchased from Invitrogen (Carlsbad, CA, USA). Gentamicin sulfate, insulin, linoleic acid, alpha-tocopherol, 3,3',5-triiodo-L-thyronine, apo-transferrin, choline chloride, hydrocortisone 21-hemisuccinate, alpha-lipoic acid and Basal Medium Eagle vitamin solution were purchased from Sigma (St Louis, MO, USA). Retinol, sodium bicarbonate, L-carnitine and vitamin B12 were purchased from Fluka Chemie AG (Buchs, Switzerland). Ammonium chloride (NH_4Cl) and roscovitine were purchased from Sigma (St Louis, MO, USA), Z-VAD-FMK methyl ester cell-permeable caspase inhibitor from Biomol (Plymouth Meeting, PA, USA). Histone H1 and protein G-Sepharose were from Sigma (St Louis, MO, USA), while ATP was from Cell Signaling (Beverly, MA, USA). L-[1-^{14}C] glutamic acid (60 mCi/mmol) was from Amersham Biosciences (Piscataway, NJ, USA) and acetyl coenzyme A[acetyl-1-^{14}C] (4 mCi/mmol) from NEN/Perkin Elmer (Boston, MA, USA).

Mouse monoclonal anti-α-fodrin antibody was purchased from Biomol (Plymouth Meeting, PA, USA). Rabbit polyclonal anti-cdk5 and anti-p35/p25 (C19) antibodies as well as mouse monoclonal anti-histone H1 and anti-neurofilament M (NF-M; clone NF-09) antibodies and goat polyclonal anti-myelin basic protein (MBP) were purchased from Santa Cruz Biotechnology (Santa Cruz, CA, USA). Mouse monoclonal anti-phosphorylated NF-M antibody (clone NN18), anti-microtubule-associated protein 2 (MAP-2), anti-glial fibrillary acidic protein (GFAP; clone GA5) and anti-galactocerebroside (GalC; clone mGalC) antibodies were purchased from Chemicon (Temecula, CA, USA). Rabbit polyclonal anti-cleaved caspase-3 (Asp175), anti-phospho-Erk1/2 and anti-total Erk1/2 antibodies were

purchased from Cell Signaling (Beverly, MA, USA) while rabbit polyclonal anti-phospho-histone H1 antibody was from Calbiochem (San Diego, CA, USA).

Reaggregated developing brain cell cultures

Rotation-mediated reaggregated cell cultures derived from fetal rat telencephalon were prepared as previously described (Honegger and Monnet-Tschudi, 2001; Braissant et al., 2002). In brief, the pooled forebrains of 15-day fetal rats (Sprague-Dawley, Harlan, Netherlands; animals handled according to the rules of the Swiss Academy for Medical Sciences) were dissociated mechanically, washed and resuspended in serum-free, chemically defined medium consisting of DMEM with high glucose (25 mM) supplemented with insulin (0.8 µM), triiodothyronine (30 nM), hydrocortisone-21-phosphate (20 nM), transferrin (1 µg/ml), biotin (4 µM), vitamin B_{12} (1 µM), linoleate (10 µM), lipoic acid (1 µM), L-carnitine (10 µM), choline chloride (2.5 g/l), sodium chloride (3.7 g/l) and trace vitamins and ions. Gentamicin sulfate (25 µg/ml) was used as an antibiotic. The cultures were incubated at 3.6 x 10^7 cells per flask and maintained under constant gyratory agitation at 37°C, in an atmosphere of 10% CO_2 and 90% humidified air. Media were replenished every 3 days from day-in-vitro (DIV 5) onward by exchanging 5 ml of medium (of a total of 8 ml) per flask. On DIV 8, culture media were recovered, immediately centrifuged to remove cell debris, and tested for lactate dehydrogenase (LDH) release. On the day of harvest (DIV 8 or DIV 13), aggregate pellets were washed three times with ice-cold PBS, embedded in Tissue-Tek O.C.T cryo-medium (Digitana, Switzerland) or frozen in liquid nitrogen and kept at -80°C until analysis.

Treatments

Cultures were exposed to ammonia (NH_4Cl, 5 mM) (Braissant et al., 1999; Braissant et al., 2002; Braissant et al., 2008) for 3 days (DIV 5-8) or 8 days (DIV 5-13). Cultures exposed to

ammonia for 3 days (DIV 5-8) were treated at DIV 5 with Z-VAD-FMK (a broad spectrum caspase inhibitor) or roscovitine (an inhibitor of cdk5). NH_4Cl stock solution was prepared in milliQ water at 170 mM. The pH and osmolarity of each media with and without NH_4Cl and inhibitors was stable at value of 7.4 and 340 mOsmol, respectively. Inhibitors were diluted in dimethyl-sulfoxide (DMSO) and the highest DMSO concentration in the culture media was 1%. The controls treated only with DMSO were assessed.

LDH release measurement

At DIV 8, media samples were assayed for LDH activity after minimal storage at 4°C. The calibrators and reagents used were provided by the manufacturer of the commercial LDH kit (Roche Diagnostics GmbH, Mannheim, Germany) and LDH activity was assessed by measuring the rate of change in absorbance at 340 nm (Modular, Hitachi). The enzymatic reaction: pyruvate + NADH + H^+ => lactate + NAD^+ is catalysed by the enzyme LDH and the oxidation of NADH results in a decrease in absorbance at 340 nm. The rate of decrease in absorbance is directly proportional to LDH activity.

Cell type-specific enzyme assays

Aggregates were homogenized in 2 mM potassium phosphate containing 1 mM EDTA (pH 6.8) using glass–glass homogenizers (Bellco). The homogenates were briefly sonicated and divided into aliquots for the different assays. Activity of choline acetyltransferase (ChAT; EC 2.3.1.6) was determined by a modification (Wilson et al., 1972) of the radioenzymatic method of Schrier and Shuster (1967) and corrected for the portion of nonspecific activity determined by omission of choline in the assay mixture. Glutamic acid decarboxylase (GAD; EC 4.1.1.15) activity was determined by a modification of the radioenzymatic method of Wingo and Wapara (1950). Glutamine synthetase (GS; EC 6.3.1.2) activity was assayed by a modification (Patel et al., 1982) of the radioenzymatic method of Pishak and Phillips (1979).

L-[1-^{14}C] glutamic acid was used as precursor, and phosphoenolpyruvate/pyruvate kinase as the ATP-regenerating system (Patel et al., 1982). The activity of 2',3'-cyclic nucleotide 3'-phosphohydrolase (CNP; EC3.1.4.37) was measured according to the spectrophotometric method of Kurihara and Tsukada (1967) using the sodium salt of adenosine-2',3'-cyclic monophosphate as the substrate.

In situ cell death detection

To detect typical features of apoptosis, nuclear DNA was stained using 4',6-diamidino-2-phenylindole (DAPI). Aggregate cryosections (16 µm) were incubated with DAPI (Molecular probes, Eugene, OR, USA) for 10 min at room temperature and then rinsed with distilled water.

In situ detection of apoptotic cell death was performed using terminal desoxynucleotidyl transferase (TdT)-mediated dUTP nick end labeling (TUNEL) on cryosections (16 µm) of aggregates. TUNEL staining was performed according to supplier recommendations using In Situ Cell Death Detection kit Fluorescein (Roche Diagnostics, Switzerland). Sections were permeabilized 2 min with 0.1% Triton X 100 at room temperature and washed with PBS. Sections were then incubated with label solution (mix of TdT from calf thymus and fluorescein-dUTP) for 1 hour at 37°C in humid chamber, resulting in green fluorescence within apoptotic cells. For negative controls, TdT was omitted resulting in no nuclear staining.

Caspase activity assay

Activities of caspase-1, -2, -3, -8 and -9 were determined using the corresponding caspase activity colorimetric assay kits from Biovision (Mountain View, CA, USA). Briefly, cells were lysed in lysis buffer containing 20 mM Tris-HCl, 150 mM NaCl, 1 mM Na_2EDTA, 1 mM EGTA, 1% Triton, 2.5 mM sodium pyrophosphate, 1 mM beta-glycerophosphate, 1 mM

Na_3VO_4 and 1 µg/ml leupeptin (Cell Signaling, Beverly, MA, USA). Supernatants were collected after centrifugation at 10'000 x *g* for 1 min. The protein concentration of each sample was determined by the bicinchoninic acid assay (BCA; Pierce, Rockford, IL, USA). In a 96-wells plate, 200 µg of total cell proteins were added to 50 µl reaction buffer containing 10 mM dithiothreitol (DTT) and 5 µl substrates of caspase-1, -2, -3, -8 and -9, *i.e* YVAD-*p*NA, VDVAD-*p*NA, DEVD-*p*NA, IETD-*p*NA, and LEHD-*p*NA, respectively (final concentration 200 µM). Samples were incubated at 37 °C for 4 h and the enzyme-catalyzed release of *p*NA was quantified at 405 nm using a Molecular Devices VersaMax microplate reader. The values of NH_4Cl-treated samples were normalized to corresponding untreated controls allowing determination of the fold increase in caspase activity.

Western blot analysis

Aggregates were homogenized in 10 mM Tris-HCl, pH 7.5, containing 6 M urea, 0.1% SDS, protease inhibitors (Complete; Roche, Switzerland) and phosphatase inhibitors (cocktail 2 aqueous solution, Sigma, St Louis, MO, USA). Homogenates were centrifuged at 16,000 x *g* for 10 min, and supernatants were recovered. Supernatant proteins were measured by BCA assay and diluted at a final concentration of 3 µg/µl in NuPage® sample buffer (0.14 M Tris base, 0.5 mM EDTA, 10 % glycerol, 2% lithium dodecyl sulphate, dithiothreitol 50 mM, pH 8.5) (Invitrogen, Carlsbad, CA, USA). Samples were heated at 70°C for 10 min and proteins were separated using NuPage 12 % Bis-Tris gels and MOPS running buffer (50 mM MOPS, 50 mM tris, 3.5 mM sodium dodecyl sulphate (SDS), 0.8 mM EDTA) at a constant voltage (200 V, 60 min), or 7% Tris-Acetate gels and Tris-Acetate running buffer (50 mM Tricine, 50 mM Tris-base, 3.5 mM SDS) at a constant voltage (150 V, 75 min). Proteins were transferred for 90 min at constant voltage (12 V) onto polyvinylidene difluoride membranes (Immobilon; Millipore, Bedford, MA, USA) under semi-dry conditions (Transblot SD semi-dry transfer cell, Biorad, Hercules, CA, USA) using Bjerrum buffer (48 mM Tris base, 39 mM glycine,

0.13 mM SDS, and 15 % methanol). Membranes were blocked with 5% non-fat dry milk in TBS-Tween (Trizma base 20 mM pH 7.6, NaCl 137 mM, 0.05% Tween). After blocking, the membranes were incubated overnight with primary antibodies diluted in 3% dry milk and TBS-T. Anti-α-fodrin and anti-p35/p25 antibodies were diluted 1:5000, while anti-phospho-histone H1, anti-cdk5, anti-NF-M (NF-09), anti-MBP, anti-phospho-NF-M (NN18), anti-phospho-Erk1/2, anti-total Erk1/2 and anti-histone H1 antibodies were diluted 1:1000. The membranes were then washed with TBS-T and probed with horseradish peroxidase conjugated goat anti-mouse IgG or goat anti-rabbit IgG (1:3500; Vector laboratories, Burlingame, CA, USA). A second wash was performed and blots were developed by chemiluminescence (ECL; Amersham Biosciences, Buckinghamshire, UK). Blots were stripped (Re-Blot Plus Mild antibody stripping solution; Chemicon, Temecula, CA, USA) and reprobed with antibody against histone H1 to demonstrate equal loading of protein in each lane. The autoradiograms (Hyperfilm ECL, Amersham Biosciences, UK) were scanned with an ImageScanner (Amersham Biosciences, UK) and processed by image analysis (ImageMaster 1D; Amersham Biosciences, UK). Data were acquired in arbitrary densitometric units and transformed to percentages of the densitometric levels obtained from scans of control samples visualized on the same blots.

Immunostaining

In-situ detection of cleaved caspase-3 in aggregates was performed with Tyramide Signal Amplification (TSA) kit (Molecular Probes, Eugene, OR, USA). Aggregate cryosections (16 µm) were postfixed 1 h in 4% paraformaldehyde (PFA) in PBS at room temperature. Sections were washed in PBS and incubated in 1 % H_2O_2 (TraceSelect 30%, Fluka Chemie AG, Buchs, Switzerland) in PBS for 10 min to quench endogenous peroxidase activity. Non-specific antibody binding sites were blocked for 1h at room temperature with the blocking buffer of the kit. The primary antibody diluted 1:100 in blocking buffer was applied to sections

overnight at 4° C. After washing, sections were incubated with a Horseradish Peroxidase (HRP) anti-rabbit IgG secondary antibody (provided by the kit) for 1h. Peroxidase staining was performed using Alexa Fluor® 555-labeled tyramide diluted at 1:200 in Amplification buffer (provided by the kit) applied to sections for 5 min. For negative controls, primary antibody was omitted resulting in no staining. Sections were then incubated overnight at 4°C with the second primary antibody directed towards MAP-2 (1:100), GFAP (1:200) and GalC (1:100) to reveal neurons, astrocytes and oligodendrocytes, respectively. After washing, sections were incubated for 1h with a secondary antibody directed towards mouse-IgG or goat-IgG and labeled with Alexa Fluor® 350 (1/200) (Molecular Probes, Eugene, OR, USA). Sections were mounted under FluorSave Reagent (Calbiochem, San diego, CA, USA).

The sections were examined and digitized by the use of an Olympus BX50 fluorescence microscope equipped with an Olympus Color View 2 camera and appropriate filter combinations for red fluorescent TRITC, green fluorescent FITC and blue fluorescent DAPI. The contrast of structures was slightly enhanced and images were superposed using image-processing software (Cell Imaging Software, Olympus). For the clarity of the merged panels of figure 3, images were artificially colored in red (activated caspase 3) and green (MAP-2, GFAP or GalC), colocalization appearing in yellow.

For *in situ* detection of total NF-M in aggregates, cryosections (16 µm) were postfixed 1 h in 4% PFA in PBS at room temperature. Sections were washed in PBS and incubated in 1 % H_2O_2 (TraceSelect 30%, Fluka Chemie AG, Buchs, Switzerland) in PBS for 10 min to quench endogenous peroxidase activity. Non-specific antibody binding sites were blocked for 1 h at room temperature with bovine serum albumin (1%) in PBS. Sections were then incubated 1 h with a primary antibody directed towards total NF-M (NF-09) and staining was then processed using the AEC Histostain-Plus kit according to the manufacturer's protocol (Zymed laboratories, San Francisco, CA, USA). Sections were mounted under glycerol.

Immunoprecipitation and cdk5 activity assay

Frozen aggregate pellets were lysed in lysis buffer (for composition see Caspases activity assay) (Cell Signaling, Berverly, MA, USA). Protein concentration was determined by BCA assay and 400 µg protein was incubated with anti-cdk5 antibody (1:100) overnight at 4°C under constant rotation. Immune complexes were incubated with 50 µl protein G-sepharose 1 h at room temperature, and washed twice with cell lysis buffer and once with kinase buffer (25 mM Tris-HCl pH 7.5, 5 mM beta-glycerophosphate, 2 mM dithiothreitol (DTT), 0.1 mM Na_3VO_4, 10 mM $MgCl_2$) (Cell signaling, Beverly, MA, USA). The washed beads were then incubated in 50 µl of kinase buffer containing 25 µg of histone H1 and 200 µM ATP at 30°C for 3h30. Samples were centrifuged for 2 min at 16,000 x *g* and 30 µl of the supernatant was mixed with NuPage® sample buffer. Samples were heated at 70°C for 10 min and proteins were separated using NuPage 12 % Bis-Tris gels and MOPS running buffer. Phosphorylated Histone H1 was revealed as described above in the western-blot section, using polyclonal anti-phosphorylated histone H1 primary antibody (1:1000). Non-phosphorylated histone H1 was not detected by this antibody. Negative control were treated identically, containing no antibody instead of cdk5 antibody.

Statistics

All data points are expressed as mean ± standard error of the mean (SEM). Experiments were considered independent in that cultures were not from the same primary preparation. Statistical difference was determined with one-way analysis of variance (ANOVA) followed by Student's *t*-test (Fig. 1, 2, 4 and 5) or by Dunnett's *post hoc* test for multiple groups (Fig. 6 and 7).

Results

Ammonia induced cell death in reaggregated developing brain cell cultures

The effect of ammonia on cell death in reaggregated developing brain cell cultures was assessed by measuring LDH release in the culture medium. Exposure to ammonia (5 mM) for 3 days, from DIV 5 to DIV 8, induced a highly significant increase in LDH release indicating high general cytotoxicity (Fig. 1A). Cell type-specific effects of ammonia were also analyzed. The activities of the following enzymes were used to determine the specific susceptibility of different cell types to ammonia exposure: GS for astrocytes, CNP for oligodendrocytes, ChAT and GAD for cholinergic and GABAergic neurons, respectively. The effect of ammonia on enzymatic activities was evaluated at DIV 13 after 8 days of ammonia exposure, rather than DIV 8, because at DIV 8 cultures were relatively undifferentiated and expressed these enzymes at low levels (data not shown). At DIV 13, CNP, ChAT and GAD activities were greatly decreased suggesting that oligodendrocytes, cholinergic and GABAergic neurons were widely affected (Fig. 1B). In contrast, GS, the astrocytic marker, was not affected by ammonia exposure (Fig. 1B).

The nuclear morphology of brain cells was evaluated with DAPI staining at DIV 8 and DIV 13. Exposure to ammonia from DIV 5 to DIV 8 or DIV 13 resulted in the appearance of numerous fragmented, brightly fluorescent apoptotic nuclei at DIV 8 and DIV 13 (Fig. 1C). Apoptotic bodies, which appear at the late stage of apoptosis, were especially numerous at DIV 13, after 8 days of ammonia exposure. In control cultures, few apoptotic cells were observed. Fragmented nuclei were stained with the TUNEL method labeling the 3’-end of DNA. In control conditions, several TUNEL-positive cells could be observed, especially at DIV 8, suggesting that spontaneous apoptosis is considerable at this stage of maturation (Fig.

1C). TUNEL-positive cells were much more numerous in cultures exposed to ammonia, both at DIV 8 and DIV 13, as compared to control cultures.

Ammonia activated caspases and calpain

Activities of caspases 1, 2, 3, 8, and 9 were significantly increased by ammonia exposure in cell lysates prepared at DIV 8 and DIV 13 (Fig. 2). The increase after ammonia exposure was more pronounced at DIV 8 than at DIV 13 (Fig. 2).

Double labeling immunofluorescent experiments were performed to reveal activated caspase-3 together with either the neuronal marker MAP-2, the astrocytic marker GFAP, or the oligodendrocytic marker GalC. Although the increase of caspase-3 activity was more pronounced after 3 days of ammonia exposure (DIV 8) (Fig. 2), double labeling assays were performed at DIV 13, after 8 days of ammonia exposure, because MAP-2 and GalC were undetectable at DIV 8 in cultures exposed to ammonia (results not shown). In untreated cultures, activated caspase-3 was expressed in nuclei of neurons (Fig. 3A), reflecting the natural caspase-3-dependent apoptosis occurring in neurons of the embryonic brain (Kuida et al., 1996). Caspase-3 was also activated in few astrocytes of control cultures (Fig. 3B), while it was absent from oligodendrocytes (Fig. 3C). Ammonia exposure induced a more intense and diffuse staining and a relocalization of activated caspase-3 from nucleus to soma and fibers (Fig. 3A-C). Moreover, activated caspase-3 staining co-localized with MAP-2 staining within cellular bodies and fibers (enlarged field in Fig. 3A), but not with GFAP (enlarged field in Fig. 3B) and GalC suggesting that ammonia activated caspase-3 within the cytoplasm of neurons but not of astrocytes and oligodendrocytes.

We next investigated the activation of calpain. α-fodrin (also known as spectrin) is an endogenous substrate for calpain and the formation of the 145/150 kDa α-fodrin breakdown products (BDPs) results from the activity of calpain. We performed western blotting to

monitor the activities of calpain following ammonia exposure from DIV 5, for 6 h to 8 days. Compared to corresponding controls, ammonia led to an early increase of calpain activity 6 h after exposure, which was maintained for 6 days; calpain activity returned to control levels after 8 days (Fig. 4A and B).

Ammonia induced the cleavage of p35 to p25, but did not alter the overall kinase activity of cdk5

We investigated the role of cdk5 together with its co-activators p35 and p25, because calpain was activated by ammonia exposure, and the cdk5/p25 complex generated by calpain is involved in neuronal cell death induced by numerous neurotoxic insults. Western blotting showed that cdk5 levels were not altered by ammonia exposure (Fig. 5A). Ammonia exposure for 3 and 8 days induced a decrease of p35 levels, paralleled with an increase in p25 levels (Fig. 5A). Together with the densitometric quantification showing an increase of the p25/p35 ratio under ammonia exposure (Fig. 5B), these results suggest that the cleavage of p35 to p25 is increased under ammonia exposure. Finally, we evaluated the effect of ammonia exposure on the overall kinase capacity of cdk5, by immunoprecipitating endogenous cdk5 protein from cell extracts and assaying its ability to phosphorylate the common cdk substrate histone H1. We showed that the overall kinase activity of cdk5 was not altered by ammonia exposure either a DIV 8 or at DIV 13 in reaggregated developing brain cell cultures (Fig. 5C).

Effect of caspases and cdk5 inhibition on ammonia-induced brain cell death

We next examined the effects of Z-VAD-fmk (a pan-caspases inhibitor) and roscovitine (a cdk5 inhibitor) on ammonia-induced cell death. We showed that roscovitine significantly reduced ammonia-induced cell death from 166 ± 3 % to 132 ± 5 % (50 µm roscovitine) and 123 ± 4 % (100 µm roscovitine; control cultures: 100 %) while Z-VAD-fmk (100 µm) was ineffective (Fig. 6A). These results indicate that cdk5 inhibition prevented half of the

ammonia-induced death of developing brain cells. Two different calpain inhibitors, PD150606 and Acetyl-Leucyl-Leucyl-Norleucinal (ALLN), were also tested but failed to inhibit calpain (data not shown), most probably because of the low concentration used (2 μM), as higher concentrations were cytotoxic.

We then investigated the activation of calpain and caspase-3 in the presence of ammonia and inhibitors, by immunodetection of the 145/150 kDa and 120 kDa BDPs of α-fodrin, illustrating calpain and caspase-3 activities, respectively (Fig 6B). We found that Z-VAD-fmk and roscovitine both inhibited caspase-3 activation and further increased calpain as compared to cultures exposed to ammonia alone (Fig. 6C and D).

Roscovitine protected the expression and phosphorylation of NF-M

We found that roscovitine protected the survival of the developing brain cells against ammonia toxicity. As p35 and p25 are neuron-specific proteins (Maccioni et al., 2001; Cheung and Ip, 2004), it is most probable that cdk5 inhibition by roscovitine protects only neurons against ammonia toxicity. We analyzed the expression level of NF-M, a neuronal marker, and of MBP, an oligodendrocyte marker, under ammonia exposure and roscovitine co-treatment. Roscovitine significantly prevented the ammonia-induced loss of NF-M expression (Fig. 7A and B). In contrast, roscovitine did not protect MBP expression, which was altered by ammonia exposure (Fig. 7A). These results suggest that roscovitine protected the survival of neurons but not of oligodendrocytes and this may explain why roscovitine did not completely prevent ammonia-induced leakage of LDH (Fig. 6A).

Moreover, roscovitine, alone or in combination with ammonia, induced NF-M hyperphosphorylation as compared to control condition (Fig. 7A and C). It was shown previously that activation of the mitogen-activated protein kinase Erk1/2 pathway results in

NF-M phosphorylation (Veeranna et al., 1998; Li et al., 1999). It was also shown that cdk5 inhibits the upstream activator of Erk1/2 and that the absence of cdk5 activity results in an increase of NF-M phosphorylation (Sharma et al., 2002). Thus, we tested in our model whether Erk1/2 activation was up-regulated by roscovitine. Western blot shows that Erk1/2 was significantly activated by roscovitine alone and in combination with ammonia (Fig. 7A and D). These results suggest that roscovitine-induced inhibition of cdk5 activated Erk1/2, which in turn increased the phosphorylation of NF-M.

Immunohistochemical staining of total NF-M in control reaggregated cell cultures revealed, at the periphery of the aggregates, the presence of NF-M-positive long fibers, which were previously identified as axons (Fig. 7E) (Honegger and Monnet-Tschudi, 2001; Braissant et al., 2002). Ammonia exposure caused the almost complete disappearance of NF-M positive fibers (Fig. 7E), confirming the axonal outgrowth inhibition previously observed (Braissant et al., 2002; see also Supplementary Figure 1). Roscovitine did not rescue NF-M positive fibers and axonal outgrowth (Fig. 7E), although the levels of NF-M were preserved as shown by immunoblotting (Fig. 7B and C). Roscovitine alone induced the inhibition of axonal outgrowth and the accumulation of NF-M within cellular bodies (Fig. 7E). Our results suggest that roscovitine allowed partial protection of brain cells survival but in the meantime inhibited the axonal outgrowth.

Discussion

Ammonia induces death of developing neurons and oligodendrocytes

Despite extensive knowledge of the effects of hyperammonemia on the adult brain, little is known about the mechanisms leading to irreversible brain lesions occurring specifically in hyperammonemic newborns and infants. Our aim was to investigate the intracellular mechanisms involved in the death of developing brain cells exposed to ammonia.

Apoptosis was induced by ammonia exposure in developing brain cell cultures, as revealed by the occurrence of apoptotic bodies, nuclear fragmentation, and caspases activation. As TUNEL not only reveals internucleosomal DNA fragmentation (associated with apoptosis) but also random DNA breakdown (associated with necrosis), ammonia exposure may also induce necrosis in our model.

Ammonia strongly affected neuron- and oligodendrocyte-specific enzymes. The decrease in cell type-specific enzyme activity was established as a sensitive indicator for neurotoxicant-induced adverse effects (Honegger and Schilter, 1992; Zurich et al., 2004). Alterations in cholinergic neurons fit with our previous results (Braissant et al., 2002) and with findings in *spf* mouse, a model of hyperammonemia caused by OTC deficiency, showing cholinergic neuronal loss in the cerebral cortex (Ratnakumari et al., 1994). The loss of oligodendrocytes is in line with clinical data showing hypomyelination in various cases of neonatal hyperammonemia (Harding et al., 1984). Ammonia exposure activated caspase-3 in neurons but not in oligodendrocytes and astrocytes, suggesting that ammonia-induced neuronal death was apoptotic, while oligodendrocytic death was caspase-3-independent. While both decrease

and increase of GS activity were shown in ammonia-exposed astrocytes (Huang et al., 1994; Leite et al., 2006), ammonia did not alter GS activity in our model.

Apoptotic neurons (and some astrocytes) were observed in untreated cultures, probably reflecting the physiological apoptosis occurring in the developing brain (Roth and D'Sa, 2001; Olney et al., 2002).

Role of caspases and calpain in ammonia-induced death of developing brain cells

Caspase-1, -2, -3, -8 and -9 were activated by ammonia exposure. Caspase-3 is an apoptosis executioner caspase while caspase-2, -8 and -9 are initiator caspases. Caspase-8 belongs to the extrinsic pathway involving death receptors, while caspase-9 is involved in the intrinsic pathway resulting from mitochondrial alterations (Rupinder et al., 2007). Our results suggest that ammonia triggers both extrinsic and intrinsic apoptotic pathways. Moreover, ammonia exposure may also induce inflammatory processes, as caspase-1 is involved in inflammation.

The increase in caspases activity was higher after 3 days than after 8 days of ammonia exposure. In adult rats, acute ammonia intoxication does not affect caspase-9 or caspase-3 activities (Kosenko et al., 2007). Taken together, both studies suggest that ammonia-induced apoptosis in brain cells depends on their level of maturation. Similarly, we previously showed that ammonia inhibits axonal growth in early developing neurons, but that axons are not altered after synaptogenesis (Braissant et al., 2002). This is also found clinically, as hyperammonemia induces irreversible brain damage in newborns and infants but not in adults (Cagnon and Braissant, 2007). This discrepancy in susceptibility to ammonia toxicity may be explained by the highly expressed apoptosis machinery in the developing brain, enabling a greater capacity and readiness to undergo apoptosis (Blomgren et al., 2007). Thus,

programmed cell death occurring in immature brain might increase the susceptibility to apoptosis induced by neurotoxicants such as ammonia.

Calpain activation started after 6 h of ammonia exposure, and lasted 6 days. Calpain activation is a common response to various neurological injuries associated with an intracellular calcium increase, which is also triggered by ammonia (Rose et al., 2005; Hillmann et al., 2007). In the brain of rats with acute hyperammonemia, MAP-2 proteolysis is due to calpain activation (Felipo et al., 1993).

The pan-caspases inhibitor (Z-VAD-fmk) effectively inhibited caspase-3 but was not neuroprotective. Z-VAD-fmk over-activated calpain, suggesting that inhibition of caspases caused a shift from caspase-induced apoptosis to calpain-induced cell death. This fits with data showing that Z-VAD-fmk blocks apoptotic cell death while sensitizing cells to necrotic cell death and autophagic cell death (Vandenabeele et al., 2006). Since inhibition of a given cell death pathway may enhance alternative ones, treatment strategies should optimally be directed at multiple targets.

Our model did not allow to examine whether calpain inhibition protects developing brain cells from ammonia toxicity, because PD150606 and ALLN were cytotoxic at concentrations capable of calpain inactivation.

Role of cyclin-dependent kinase 5

Because ammonia increased calpain activity, we investigated whether its potential target p35 was cleaved to p25. The conversion of p35 to p25 has been observed in neuronal death induced by amyloid-β peptide, glutamate excitotoxicity, DNA damage, endoplasmic reticulum stress, increase of calcium intracellular levels and in a model of HIV neurotoxicity

(Patrick et al., 1999; Lee et al., 2000; O'Hare et al., 2005; Jamsa et al., 2006; Saito et al., 2007; Wang et al., 2007). p35 contains a signal motif anchoring cdk5/p35 complex to the cell membrane, while the conversion of p35 to p25 liberates the cdk5/p25 complex into the cytoplasm. It was suggested that cdk5/p25 translocates to the nucleus, and that the cdk5/p25 nuclear accumulation contributes to neuronal death (O'Hare et al., 2005; Saito et al., 2007). We showed that in the presence of ammonia, p35 level decreased while p25 accumulated, suggesting cdk5/p25 involvement in ammonia-induced neuronal death. As we also showed that ammonia exposure did not change the overall kinase capacity of cdk5, it suggests that ammonia exposure diverted part of cdk5 kinase activity from its p35-associated, neuronal maturation roles, to the p25-associated neuronal death pathway. The nuclear phosphorylation of the tumor suppressor protein p53 by cdk5/p25 was recently suggested to mediate neuronal apoptosis (Lee et al., 2007). Whether or not p53 is involved in ammonia-induced death of developing brain cells remains to be determined.

Here we report that roscovitine decreased the death of developing brain cells, suggesting an important role for cdk5 in ammonia-induced cell death. Neuroprotection through the inhibition of cdk5 activity was previously observed in endoplasmic reticulum-stressed neurons and in neurons treated with amyloid β peptide (Zheng et al., 2005; Saito et al., 2007). Roscovitine inhibited caspase-3 activation, suggesting that cdk5/p25 is an upstream regulator of caspase-3 (Fig. 8). On the other hand, as described above for pan-caspases inhibitor Z-VAD-fmk, roscovitine activated calpain, confirming that caspase-3 inhibition causes a shift to caspase-independent cell death (Kroemer and Martin, 2005; Vandenabeele et al., 2006). However, as calpain is an upstream regulator of cdk5/p25, calpain over-activation may have only limited effects on neuronal cell death when cdk5 is inhibited by roscovitine (Fig. 8).

Roscovitine protected the level of NF-M, a neuron-specific marker, but not those of MBP, an oligodendrocyte-specific marker. This suggests that roscovitine protected neurons but not oligodendrocytes against ammonia toxicity, a predictable result since cdk5/p35 and cdk5/p25 are neuron-specific. This may explain why roscovitine did not completely prevent ammonia-induced LDH leakage.

While cdk5 can phosphorylate NF-M (Kesavapany et al., 2003; Shea et al., 2004), we showed that cdk5 inhibition by roscovitine induced NF-M hyperphosphorylation. Cdk5 activation can inhibit MEK1, the upstream activator of Erk1/2 (Sharma et al., 2002; Moran et al., 2005), while Erk1/2 can directly phosphorylate NF-M (Li et al., 1999). Since roscovitine activated Erk1/2, it suggests that NF-M hyperphosphorylation observed under roscovitine treatment is due to Erk1/2 activation. In line with this, $p35^{-/-}$ mice, lacking cdk5 activity, show NF-M hyperphosphorylation and enhanced Erk1/2 phosphorylation (Sharma et al., 2002; Hallows et al., 2003)

Roscovitine alone impaired axonal outgrowth and induced NF-M accumulation within neuronal soma. The latter was also observed in $cdk5^{-/-}$ mice (Sharma et al., 2002). This inhibitory effect on neurite outgrowth is probably due to cdk5/p35 inhibition by roscovitine, since roscovitine does not specifically inhibit cdk5/p25 (Fig. 8). Indeed, despite ammonia exposure and the p25 generation, cdk5/p35, which plays crucial roles in axonal elongation and maintenance (Nikolic et al., 1996; Harada et al., 2001; Hahn et al., 2005), is still present. Therefore, specific inhibition of cdk5/p25 without inhibiting cdk5/p35 would be of great interest to protect neuronal cells from ammonia toxicity without inhibiting neurite outgrowth.

Neuronal death in neurodegenerative diseases and experimental stress conditions has been attributed to an attempt by post-mitotic neurons to re-enter the cell cycle, which is mediated

by cdks other than cdk5 (Herrup and Yang, 2007). As roscovitine can also inhibit cdk1 and cdk2 (Meijer et al., 1997; Bach et al., 2005), the protective effects of roscovitine may also be mediated by inhibition of other cdks. Further experiments will tell whether re-entry in the cell cycle and concomitant activation of cdks are involved in ammonia-induced death of developing brain cells.

Conclusion

Our data contribute to elucidate some of the ammonia-induced death pathways in the developing brain, and may also suggest the development of therapeutic strategies to protect hyperammonemic newborns and infants from neuronal death. However, before claiming cdk5 as a potential therapeutic target, more work is clearly needed to assess whether the over-activation of cdk5/p25 is also involved in ammonium-induced neuronal death *in vivo*.

Acknowledgements

The authors thank Marc Loup and Denise Tavel for their excellent technical assistance, as well as Paul Honegger for his critical reading of the manuscript and his help with the reaggregated brain cell cultures. This work was supported by the Swiss National Science Foundation, Grants n° 3100-063892, 3100A0-1000778 and 3100A0-116859.

References

Bach, S., Knockaert, M., Reinhardt, J., Lozach, O., Schmitt, S., Baratte, B., Koken, M., Coburn, P., Tang, L., Jiang, T., Liang, D., Galons, H., Dierick, J.F., Pinna, L.A., Meggio, F., Totzke, F., Schächtele, C., Lerman, A.S., Carnero, A., Wan, Y., Gray, N., Meijer, L., 2005. Roscovitine targets, protein kinases and pyridoxal kinase. J. Biol. Chem. 280, 31208-31219.

Blomgren, K., Zhu, C., Wang, X., Karlsson, J.O., Leverin, A.L., Bahr, B.A., Mallard, C., Hagberg, H., 2001. Synergistic activation of caspase-3 by m-calpain after neonatal hypoxia-ischemia: a mechanism of "pathological apoptosis"? J. Biol. Chem. 276, 10191-10198.

Blomgren, K., Leist, M., Groc, L., 2007. Pathological apoptosis in the developing brain. Apoptosis 12,993-1010.

Braissant, O., Honegger, P., Loup, M., Iwase, K., Takiguchi, M., Bachmann, C., 1999. Hyperammonemia: regulation of argininosuccinate synthetase and argininosuccinate lyase genes in aggregating cell cultures of fetal rat brain. Neurosci. Lett. 266, 89-92.

Braissant, O., Henry, H., Villard, A.M., Zurich, M.G., Loup, M., Eilers, B., Parlascino, G., Matter, E., Boulat, O., Honegger, P., Bachmann, C., 2002. Ammonium-induced impairment of axonal growth is prevented through glial creatine. J. Neurosci. 22, 9810-9820.

Braissant, O., Cagnon, L., Monnet-Tschudi, F., Speer, O., Wallimann, T., Honegger, P., Henry, H., 2008. Ammonium alters creatine transport and synthesis in a 3D-culture of developing brain cells, resulting in secondary cerebral creatine deficiency. Eur. J. Neurosci. 27, 1673-1685.

Cagnon, L., Braissant, O., 2007. Hyperammonemia-induced toxicity for the developing central nervous system. Brain. Res. Rev. 56, 183-197.

Cheung, Z.H., Ip, N.Y., 2004. Cdk5: mediator of neuronal death and survival. Neurosci. Lett. 361, 47-51.

Enns, G.M., Berry, S.A., Berry, G.T., Rhead, W.J., Brusilow, S.W., Hamosh, A., 2007. Survival after treatment with phenylacetate and benzoate for urea-cycle disorders. N. Engl. J. Med. 356, 2282-2292.

Felipo, V., Grau, E., Minana, M.D., Grisolia, S., 1993. Ammonium injection induces an N-methyl-D-aspartate receptor-mediated proteolysis of the microtubule-associated protein MAP-2. J. Neurochem. 60, 1626-1630.

Gropman, A.L., Summar, M., Leonard, J.V., 2007. Neurological implications of urea cycle disorders. J. Inherit. Metab. Dis. 30, 865-879.

Hahn, C.M., Kleinholz, H., Koester, M.P., Grieser, S., Thelen, K., Pollerberg, G.E., 2005. Role of cyclin-dependent kinase 5 and its activator P35 in local axon and growth cone stabilization. Neuroscience 134, 449-465.

Hallows, J.L., Chen, K., DePinho, R.A., Vincent, I., 2003. Decreased cyclin-dependent kinase 5 (cdk5) activity is accompanied by redistribution of cdk5 and cytoskeletal proteins and increased cytoskeletal protein phosphorylation in p35 null mice. J. Neurosci. 23, 10633-10644.

Harada, T., Morooka, T., Ogawa, S., Nishida, E., 2001. ERK induces p35, a neuron-specific activator of Cdk5, through induction of Egr1. Nat. Cell. Biol. 3, 453-459.

Harding, B.N., Leonard, J.V., Erdohazi, M., 1984. Ornithine carbamoyl transferase deficiency: a neuropathological study. Eur. J. Pediatr. 141, 215-220.

Herrup, K., Yang, Y., 2007. Cell cycle regulation in the postmitotic neuron: oxymoron or new biology? Nat. Rev. Neurosci. 8, 368-378.

Hillmann, P., Kose, M., Sohl, K., Muller, C.E., 2007. Ammonium-induced calcium mobilization in 1321N1 astrocytoma cells. Toxicol. Appl. Pharmacol. 227, 36-47.

Honegger, P., Monnet-Tschudi, F., 2001. Aggregating neural cell culture. In: Fedoroff, S., Richardson, E. (Eds.), Protocols for neural cell culture. Humana Press Inc., Totowa NJ, pp. 199-218.

Honegger, P., Schilter, B., 1992. Serum-free aggregate cultures of fetal rat brain and liver cells: methodology and some practical applications in neurotoxicology. In: Zbinden, G.

(Ed.), The brain in bits and pieces. In vitro techniques in neurobiology, neuropharmacology and neurotoxicology, MTC Verlag, Zollikon, Switzerland, pp. 51-79.

Huang, R., Kala, G., Murthy, R.K., Hertz, L., 1994. Effects of chronic exposure to ammonia on glutamate and glutamine interconversion and compartmentation in homogeneous primary cultures of mouse astrocytes. Neurochem. Res. 19, 257-265.

Jamsa, A., Backstrom, A., Gustafsson, E., Dehvari, N., Hiller, G., Cowburn, R.F., Vasange, M., 2006. Glutamate treatment and p25 transfection increase Cdk5 mediated tau phosphorylation in SH-SY5Y cells. Biochem. Biophys. Res. Commun. 345, 324-331.

Kesavapany, S., Li, B.S., Pant, H.C., 2003. Cyclin-dependent kinase 5 in neurofilament function and regulation. Neurosignals 12, 252-264.

Klejman, A., Wegrzynowicz, M., Szatmari, E.M., Mioduszewska, B., Hetman, M., Albrecht, J., 2005. Mechanisms of ammonia-induced cell death in rat cortical neurons: roles of NMDA receptors and glutathione. Neurochem. Int. 47, 51-57.

Kosenko, E., Kaminsky, Y., Solomadin, I., Marov, N., Venediktova, N., Felipo, V., Montoliu, C., 2007. Acute ammonia neurotoxicity in vivo involves increase in cytoplasmic protein P53 without alterations in other markers of apoptosis. J. Neurosci. Res. 85, 2491-2499.

Kroemer, G., Martin, S.J., 2005. Caspase-independent cell death. Nat. Med. 11, 725-730.

Kuida, K., Zheng, T.S., Na, S., Kuan, C., Yang, D., Karasuyama, H., Rakic, P., Flavell, R.A., 1996. Decreased apoptosis in the brain and premature lethality in CPP32-deficient mice. Nature 384, 368-372.

Kurihara, T., Tsukada, Y., 1967. The regional and subcellular distribution of 2',3'-cyclic nucleotide 3'-phosphohydrolase in the central nervous system. J. Neurochem. 14, 1167-1174.

Lee, J.H., Kim, H.S., Lee, S.J., Kim, K.T., 2007. Stabilization and activation of p53 induced by Cdk5 contributes to neuronal cell death. J. Cell Sci. 120, 2259-2271.

Lee, M.S., Kwon, Y.T., Li, M., Peng, J., Friedlander, R.M., Tsai, L.H., 2000. Neurotoxicity induces cleavage of p35 to p25 by calpain. Nature 405,360-364.

Leite, M.C., Brolese, G., de Almeida, L.M., Pinero, C.C., Gottfried, C., Goncalves, C.A., 2006. Ammonia-induced alteration in S100B secretion in astrocytes is not reverted by creatine addition. Brain Res. Bull. 70, 179-185.

Li, B.S., Veeranna, Gu, J., Grant P., Pant, H.C., 1999. Activation of mitogen-activated protein kinases (Erk1 and Erk2) cascade results in phosphorylation of NF-M tail domains in transfected NIH 3T3 cells. Eur. J. Biochem. 262, 211-217.

Maccioni, R.B., Otth, C., Concha, I.I., Munoz, J.P., 2001. The protein kinase Cdk5. Structural aspects, roles in neurogenesis and involvement in Alzheimer's pathology. Eur. J. Biochem. 268, 1518-1527.

McCollum, A.T., Nasr, P., Estus, S., 2002. Calpain activates caspase-3 during UV-induced neuronal death but only calpain is necessary for death. J. Neurochem. 82, 1208-1220.

Meijer, L., Borgne, A., Mulner, O., Chong, J.P., Blow, J.J., Inagaki, N., Inagaki, M., Delcros, J.G., Moulinoux, J.P., 1997. Biochemical and cellular effects of roscovitine, a potent and selective inhibitor of the cyclin-dependent kinases cdc2, cdk2 and cdk5. Eur. J. Biochem. 243, 527-536.

Moran, C.M., Donnelly, M., Ortiz, D., Pant, H.C., Mandelkow, E.M., Shea, T.B., 2005. Cdk5 inhibits anterograde axonal transport of neurofilaments but not that of tau by inhibition of mitogen-activated protein kinase activity. Brain Res. Mol. Brain Res. 134, 338-344.

Mouatt-Prigent, A., Karlsson, J.O., Agid, Y., Hirsch, E.C., 1996. Increased M-calpain expression in the mesencephalon of patients with Parkinson's disease but not in other neurodegenerative disorders involving the mesencephalon: a role in nerve cell death? Neuroscience 73, 979-987.

Nikolic, M., Dudek, H., Kwon, Y.T., Ramos, Y.F., Tsai, L.H., 1996. The cdk5/p35 kinase is essential for neurite outgrowth during neuronal differentiation. Genes Dev. 10, 816-825.

O'Hare, M.J., Kushwaha, N., Zhang, Y., Aleyasin, H., Callaghan, S.M., Slack, R.S., Albert, P.R., Vincent, I., Park, D.S., 2005. Differential roles of nuclear and cytoplasmic cyclin-dependent kinase 5 in apoptotic and excitotoxic neuronal death. J. Neurosci. 25, 8954-8966.

Olney, J.W., Wozniak, D.F., Jevtovic-Todorovic, V., Farber, N.B., Bittigau, P., Ikonomidou, C., 2002. Drug-induced apoptotic neurodegeneration in the developing brain. Brain Pathol. 12, 488-498.

Patel, A.J., Hunt, A., Gordon, R.D., Balazs, R., 1982. The activities in different neural cell types of certain enzymes associated with the metabolic compartmentation glutamate. Brain Res. 256, 3-11.

Patrick, G.N., Zukerberg, L., Nikolic, M., de La Monte, S., Dikkes, P., Tsai, L.H., 1999. Conversion of p35 to p25 deregulates Cdk5 activity and promotes neurodegeneration. Nature 402, 615-622.

Pishak, M.R., Phillips, A.T., 1979. A modified radioisotopic assay for measuring glutamine synthetase activity in tissue extracts. Anal. Biochem. 94, 82-88.

Rajgopal, Y., Vemuri, M.C., 2002. Calpain activation and alpha-spectrin cleavage in rat brain by ethanol. Neurosci. Lett. 321, 187-191.

Ratnakumari, L., Qureshi, I.A., Butterworth, R.F., 1994. Evidence for cholinergic neuronal loss in brain in congenital ornithine transcarbamylase deficiency. Neurosci. Lett. 178, 63-65.

Raynaud, F., Marcilhac, A., 2006. Implication of calpain in neuronal apoptosis. A possible regulation of Alzheimer's disease. FEBS J. 273, 3437-3443.

Rose, C., Kresse, W., Kettenmann, H., 2005. Acute insult of ammonia leads to calcium-dependent glutamate release from cultured astrocytes, an effect of pH. J. Biol. Chem. 280, 20937-20944.

Roth, K.A., D'Sa, C., 2001. Apoptosis and brain development. Ment. Retard. Dev. Disabil. Res. Rev. 7, 261-266.

Rupinder, S.K., Gurpreet, A.K., Manjeet, S., 2007. Cell suicide and caspases. Vascul. Pharmacol. 46, 383-393.

Saito, T., Konno, T., Hosokawa, T., Asada, A., Ishiguro, K., Hisanaga, S., 2007. p25/cyclin-dependent kinase 5 promotes the progression of cell death in nucleus of endoplasmic reticulum-stressed neurons. J. Neurochem. 102, 133-140.

Schrier, B.K., Shuster, L., 1967. A simplified radiochemical assay for choline acetyltransferase. J. Neurochem. 14, 977-985.

Sharma, P., Veeranna, Sharma, M., Amin, N.D., Sihag, R.K., Grant, P., Ahn, N., Kulkarni, A.B., Pant, H.C., 2002. Phosphorylation of MEK1 by cdk5/p35 down-regulates the mitogen-activated protein kinase pathway. J. Biol. Chem. 277, 528-534.

Shea, T.B., Yabe, J.T., Ortiz, D., Pimenta, A., Loomis, P., Goldman, R.D., Amin, N., Pant, H.C., 2004. Cdk5 regulates axonal transport and phosphorylation of neurofilaments in cultured neurons. J. Cell. Sci. 117, 933-941.

Vandenabeele, P., Vanden Berghe, T., Festjens, N., 2006. Caspase inhibitors promote alternative cell death pathways. Sci. STKE. 2006, pe44.

Veeranna, Amin, N.D., Ahn, N.G., Jaffe, H., Winters, C.A., Grant, P., Pant, H.C., 1998. Mitogen-activated protein kinases (Erk1,2) phosphorylate Lys-Ser-Pro (KSP) repeats in neurofilament proteins NF-H and NF-M. J. Neurosci. 18, 4008-4021.

Wang, Y., White, M.G., Akay, C., Chodroff, R.A., Robinson, J., Lindl, K.A., Dichter, M.A., Qian, Y., Mao, Z., Kolson, D.L., Jordan-Sciutto, K.L., 2007. Activation of cyclin-dependent kinase 5 by calpains contributes to human immunodeficiency virus-induced neurotoxicity. J. Neurochem. 103, 439-455.

Widmer, R., Kaiser, B., Engels, M., Jung, T., Grune, T., 2007. Hyperammonemia causes protein oxidation and enhanced proteasomal activity in response to mitochondria-mediated oxidative stress in rat primary astrocytes. Arch. Biochem. Biophys. 464, 1-11.

Wilson, S.H., Schrier, B.K., Farber, J.L., Thompson, E.J., Rosenberg, R.N., Blume, A.J., Nirenberg, M.W., 1972. Markers for gene expression in cultured cells from the nervous system. J. Biol. Chem. 247, 3159-3169.

Wingo, W.J., Waparam, J., 1950. Decarboxylation of L-glutamic acid by brain. J. Biol. Chem. 187, 267-271.

Yang, L., Omori, K., Omori, K., Otani, H., Suzukawa, J., Inagaki, C., 2003. $GABA_C$ receptor agonist suppressed ammonia-induced apoptosis in cultured rat hippocampal neurons by restoring phosphorylated BAD level. J. Neurochem. 87, 791-800.

Yang, L., Omori, K., Suzukawa, J., Inagaki, C., 2004. Calcineurin-mediated BAD Ser155 dephosphorylation in ammonia-induced apoptosis of cultured rat hippocampal neurons. Neurosci. Lett. 357, 73-75.

Zheng, Y.L., Kesavapany, S., Gravell, M., Hamilton, R.S., Schubert, M., Amin, N., Albers, W., Grant, P., Pant, H.C., 2005. A Cdk5 inhibitory peptide reduces tau hyperphosphorylation and apoptosis in neurons. EMBO J. 24, 209-220.

Zurich, M.G., Honegger, P., Schilter, B., Costa, L.G., Monnet-Tschudi, F., 2004. Involvement of glial cells in the neurotoxicity of parathion and chlorpyrifos. Toxicol. Appl. Pharmacol. 201, 97-104.

Figure legends

Figure 1. Neurotoxic effects of ammonia exposure on reaggregated developing brain cell cultures. A: Cultures were exposed to ammonia (5 mM) for 3 days (DIV 5-8) and neurotoxicity was assessed by measurement of LDH release as a marker of cell death. The values represent the mean ± SEM from 9 replicate cultures from 3 independent experiments. *t*-test: *** $p< 0.001$ as compared to controls. **B**: Neurotoxicity was assessed after 8 days of ammonia exposure (DIV 5-13) for each cell type by measurement of GS, CNP, ChAT and GAD activities as markers of astrocytes, oligodendrocytes, cholinergic and GABAergic neurons, respectively. The values represent the mean ± SEM from at least 3 replicate cultures. In untreated cultures, the following values were found: GS activity: 57.04 ± 4.2 nmol/mg protein; CNP activity: 1.28 ± 0.12 µmol/mg protein; ChAT activity: 87 ± 6.2 pmol/mg protein and GAD activity: 267 ± 35 pmol/mg protein. *t*-test: * $p< 0.05$ and ** $p< 0.01$ as compared to controls. **C**: Nuclei were stained with DAPI, and TUNEL assay was performed, to compare nuclear fragmentation, appearance of apoptotic bodies and DNA cleavage between ammonia-exposed and control cultures. Scale bar = 50 µm.

Figure 2. Temporal changes in caspases activities after 3 and 8 days of ammonia exposure. Activities of caspase-1, -2, -3, -8 and -9 were measured using a colorimetric assay kit. Absorbances at 400 nm are expressed as percentage of control. The values represent the mean ± SEM from 5 and 9 replicate cultures for 3 days (DIV 5-8) and 8 days (DIV 5-13) of ammonia exposure, respectively. Samples were taken from 3 independent experiments. *t*-test: ***$p< 0.001$ as compared to controls after 3 days; $^{\#\#}$ $p< 0.01$ and $^{\#\#\#}$ $p<0.001$ as compared to controls after 8 days.

Figure 3. Cleaved caspase-3 accumulation within the cytoplasm of neurons under ammonia exposure. Untreated cultures and cultures exposed to ammonia for 8 days (DIV 5-13) were fixed and immunostained for cleaved (i.e., activated) caspase-3 (red signal), and co-labeled (green signal) for MAP-2 (staining of neurons, **A**), GFAP (staining of astrocytes, **B**) or GalC (staining of olidodendrocytes, **C**). Main panels show the overlay of both signals, with double-stained cells indicated by arrows or shown in enlarged fields. **D**: Controls of specificity for the anti-cleaved caspase 3 antibody. Immunostaining of control cultures with omission of the anti-cleaved caspase 3 primary antibody, and of cleaved caspase 3 in cultures exposed to ammonia and co-treated with Z-VAD-fmk, a pan-caspases inhibitor. Scale bar = 50 µm.

Figure 4. Time course analysis of α-fodrin cleavage after 8 days of ammonia exposure. **A**: Representative western blot showing the levels of intact α-fodrin (240 kDa) as well as of the 145/150 kDa α-fodrin breakdown products (BDPs; illustrating calpain activity) from whole-cell lysates of cultures after ammonia exposure. **B**: Data quantification of western blots for the 145/150 kDa BDPs. The levels of the 145/150 kDa BDPs are expressed as the percentage of respective controls. The values represent the mean ± SEM from 4 replicate cultures taken from 2 independent experiments. *t*-test: ** $p< 0.01$ and *** $p< 0.001$ as compared to corresponding control.

Figure 5. Expression of p35 and p25 after 3 and 8 days of ammonia exposure. A: Representative western blots showing the relative levels of p35, p25 and total cdk5 in whole cell lysates of control cultures and cultures exposed to ammonia (5mM) for 3 and 8 days. Histone H1 was used as loading control. **B**: Densitometric quantification of p35 cleavage to p25 (p25/p35 ratio) expressed as means ± SEM from 7 replicate cultures taken from 3

independent experiments. *t*-test: *** $p<0.001$ and $^{\#\#\#}$ $p< 0.001$ as compared to control after 3 and 8 days of ammonia exposure, respectively. (**C**) Western blot and densitometric analysis of phospho-histone H1, used for monitoring cdk5 activity.

Figure 6. Effects of caspases and cdk5 inhibitors on ammonia-induced cell death and on the activity of caspase-3 and calpain. Cultures were exposed to ammonia (5 mM) for 3 days (DIV 5-8) in the presence of the vehicle only (DMSO 1%), the pan-caspases inhibitor Z-VAD-fmk (100 µM) or the cdk5 inhibitor roscovitine (10 to 100 µM). **A**: LDH release is expressed as percentage of control cultures; every cultures contained the same amount of cells at DIV 0. A dose-response curve was performed for roscovitine exposure, 50 µM being chosen for all the following experiments. The values represent the mean ± SEM from at least 5 replicate cultures taken from 2 independent experiments. *** $p< 0.001$ compared to control and ^{ooo} $p<0.001$ compared to ammonia (one-way ANOVA followed by Dunnett's *post hoc* comparison). **B**: Representative western blot showing relative levels of α-fodrin and breakdown products (BDPs) from whole-cell lysates of cultures exposed to ammonia and inhibitors for 3 days (roscovitine: 50 µM). **C** and **D**: Quantification of the western blot presented in B. The levels of the 145/150 (C) and 120 (D) kDa BDPs, respectively illustrating calpain and caspase 3 activities, are expressed as the percentage of total α-fodrin-related immunoreactivity (sum of densitometry values of 240 kDa, 145/150 kDa and 120 kDa bands) to correct for minor differences in total protein loading from different samples. The values represent the mean ± SEM from 4 replicate cultures taken from 2 independent experiments. * $p< 0.05$ and *** $p< 0.001$ as compared to control; ^{oo} $p<0.01$ and ^{ooo} $p< 0.001$ as compared to ammonia (one-way ANOVA followed by Dunnett's *post hoc* comparison).

Figure 7. Protection of NF-M, NF-M hyperphosphorylation and activation of Erk1/2 by roscovitine. Cultures were exposed for 3 days to ammonia (5 mM) in the presence of the vehicle (DMSO 1%) or roscovitine (50 µM). **A**: Representative western blot showing MBP, total NF-M, phosphorylated NF-M, phosphorylated and total Erk1/2. Histone H1 was used as loading control. **B, C** and **D**: Densitometric analysis of total NF-M expression, phosphorylation level of NF-M (ratio of phospho-NF-M on total NF-M) and level of Erk1/2 activation (ratio of phospho-Erk1/2 on total Erk1/2), respectively. The values represent the mean ± SEM from 6 replicate cultures taken from 2 independent experiments. * $p<0.05$, ** $p<0.01$ and *** $p< 0.001$ as compared to control and ^{ooo} $p< 0.001$ as compared to ammonia (one-way ANOVA followed by Dunnett's *post hoc* comparison). **E**: Immunostaining of total NF-M revealed that axonal outgrowth is not protected by roscovitine and that roscovitine causes NF-M accumulation within the perikaryon. Scale bar = 50 µm.

Figure 8. Proposed intracellular mechanisms leading to neuronal cell death under ammonia exposure. Ammonia induces calpain activation, which can induce directly neuronal death. Activated calpain can also cleave p35 to p25 and activate caspase-3, causing neuronal death. Roscovitine can reduce neuronal death by inhibiting cdk5/p25 and the subsequent caspase-3 activation. In parallel, roscovitine also inhibits axonal growth through inhibition of cdk5/p35.

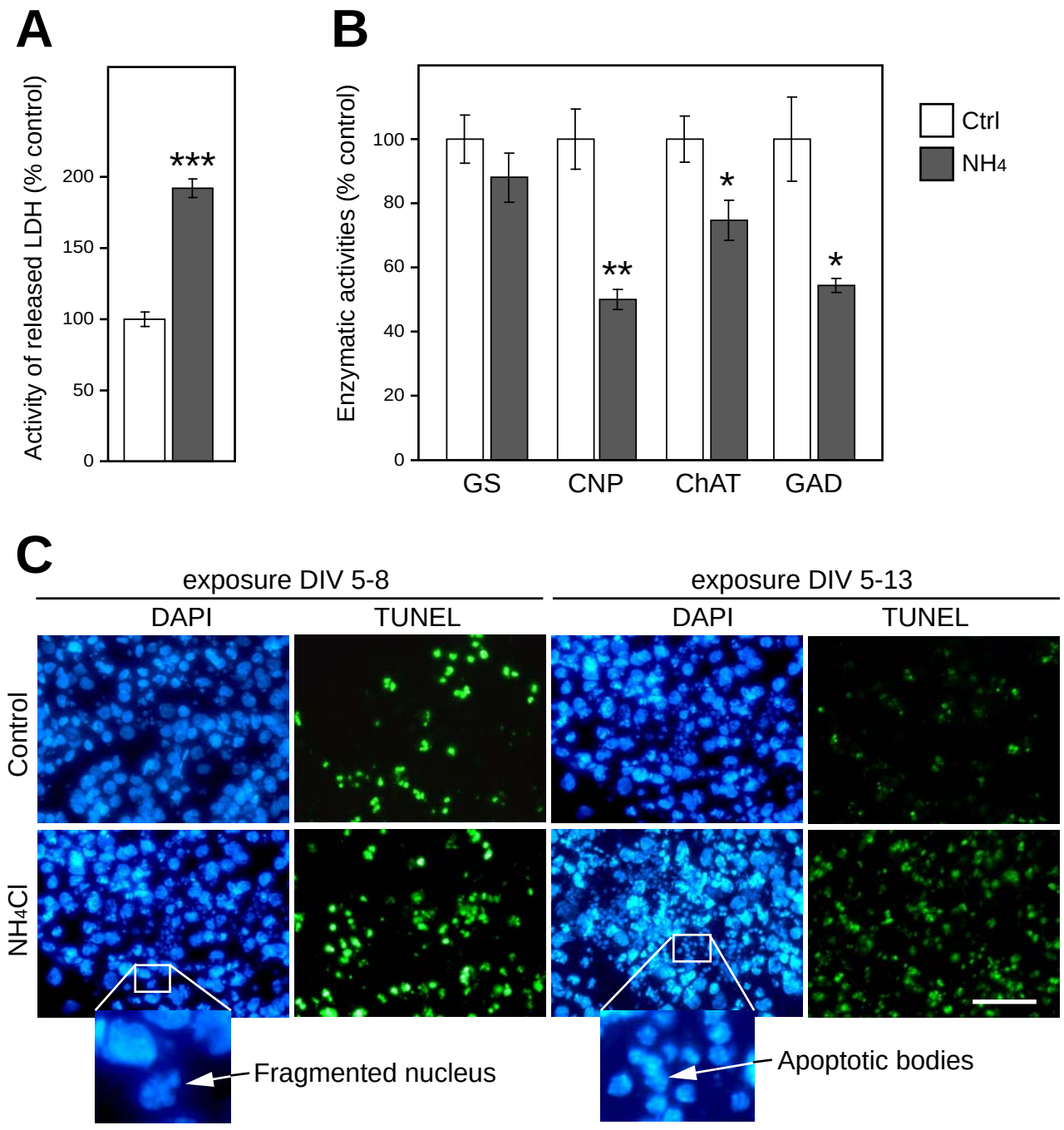

Cagnon & Braissant,
Figure 1

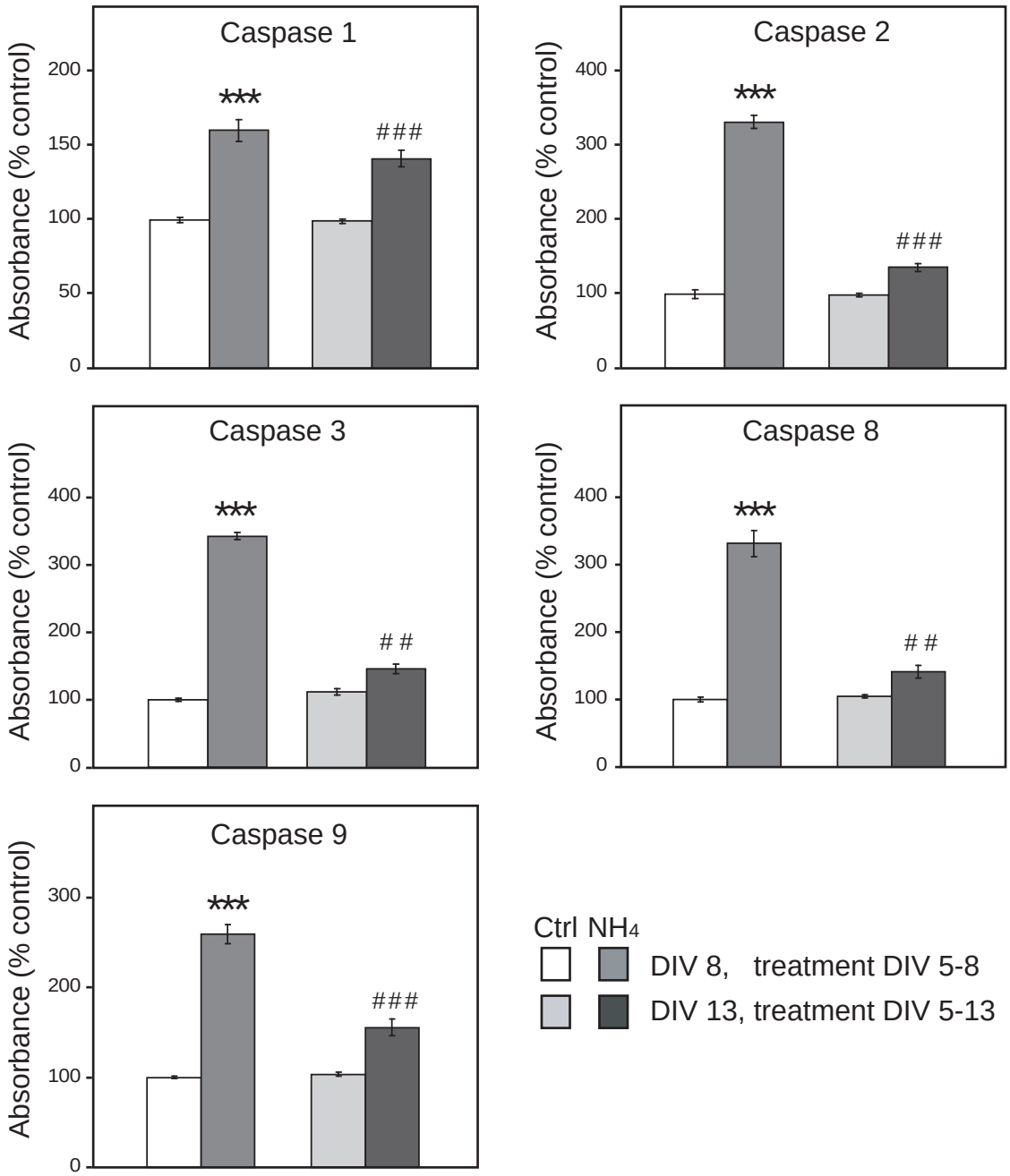

Cagnon & Braissant,
Figure 2

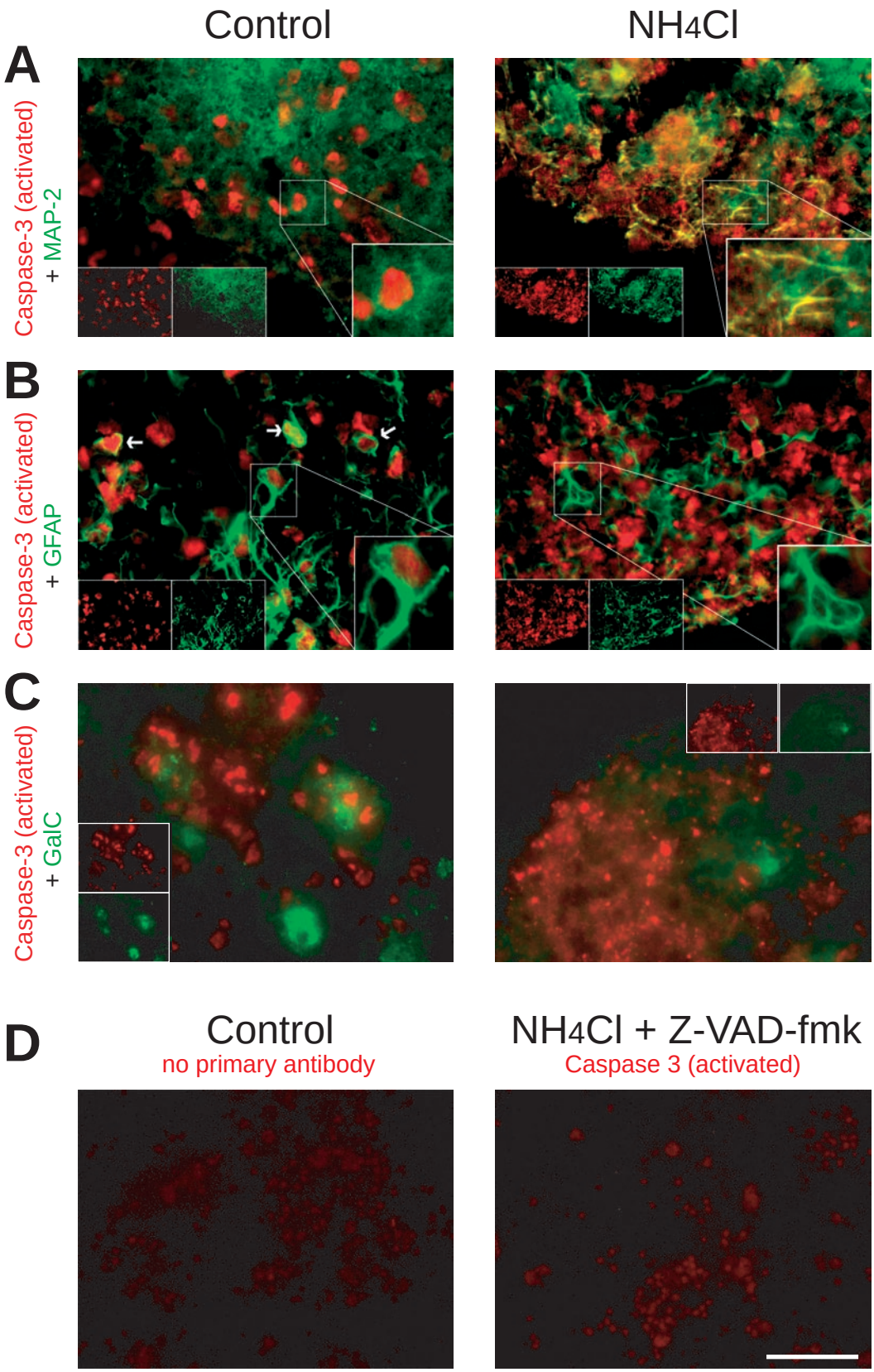

Cagnon & Braissant,
Figure 3

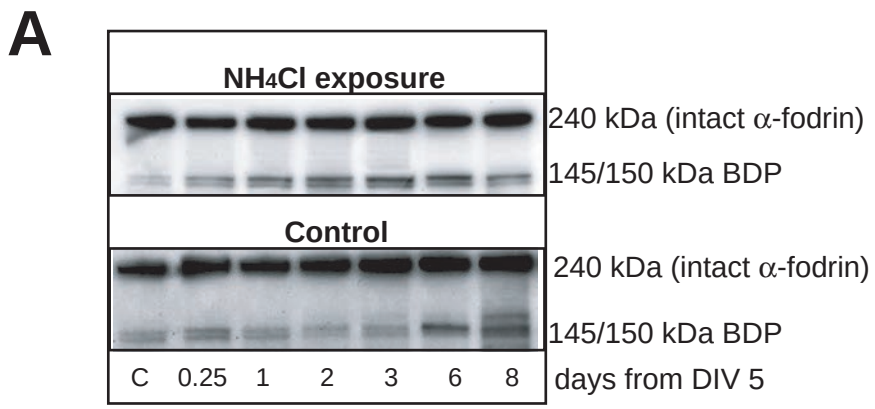

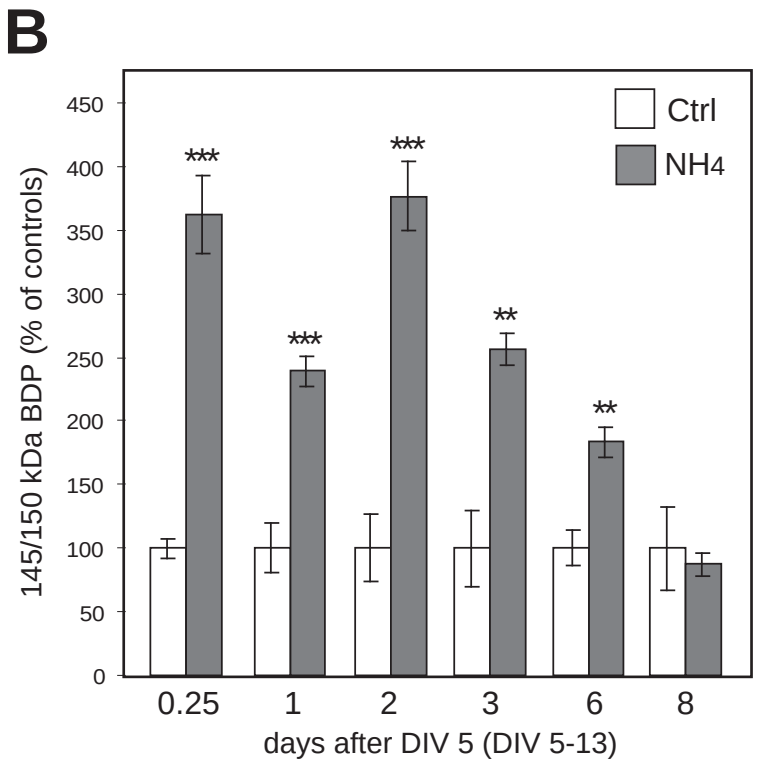

Cagnon & Braissant,
Figure 4

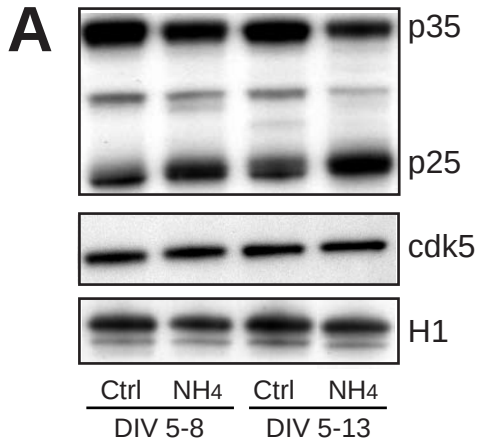

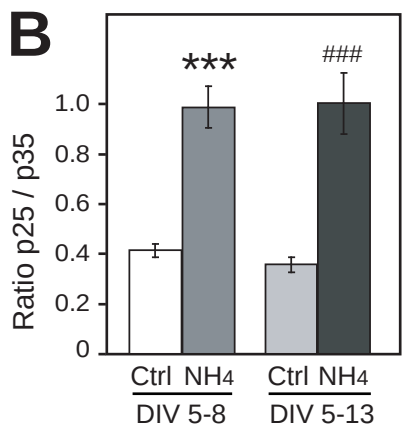

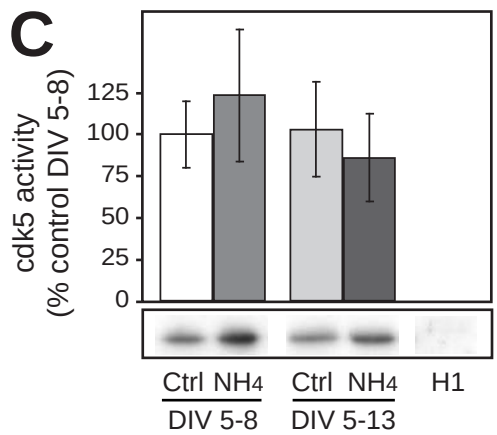

Cagnon & Braissant,
Figure 5

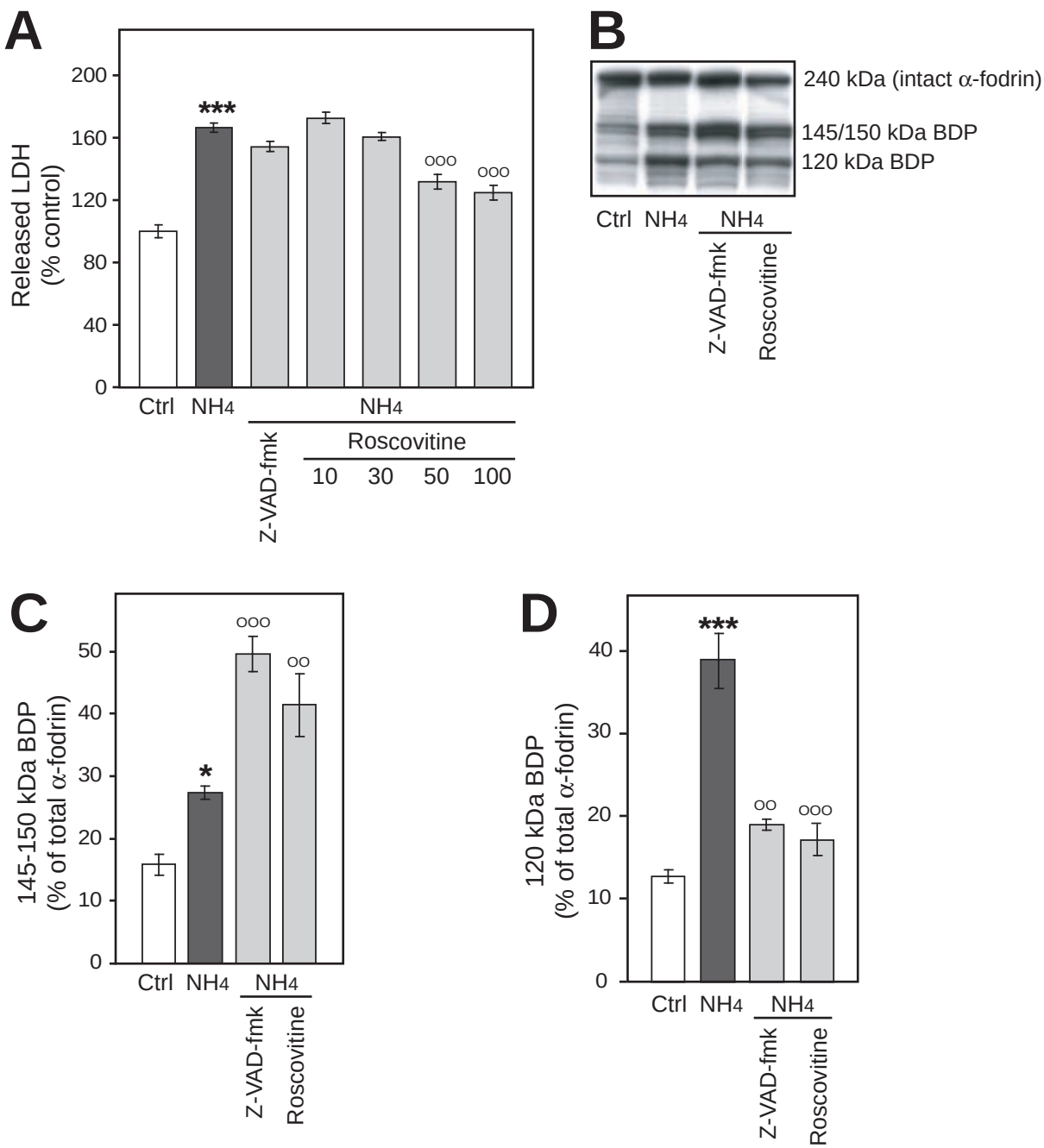

Cagnon & Braissant,
Figure 6

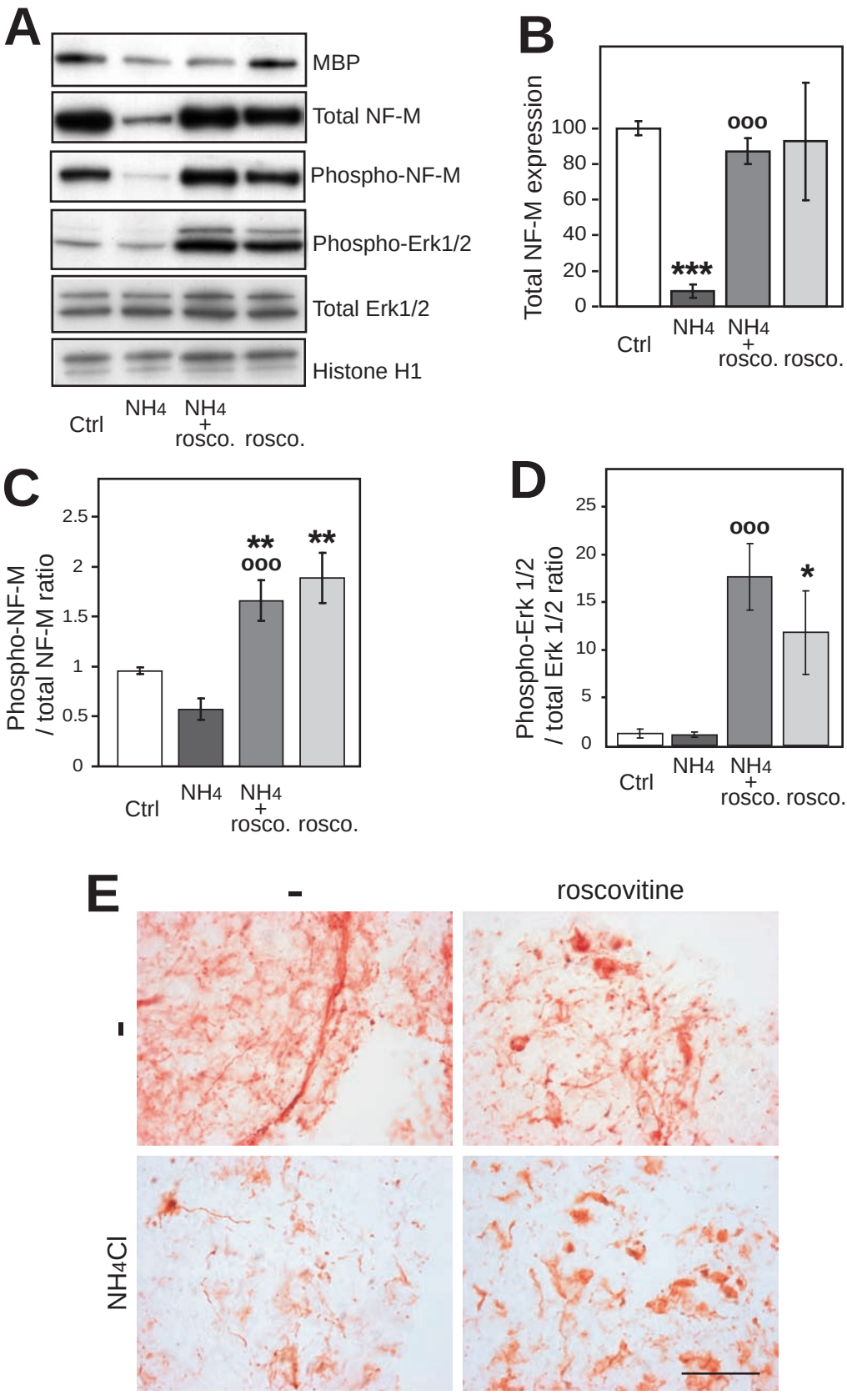

Cagnon & Braissant,
Figure 7

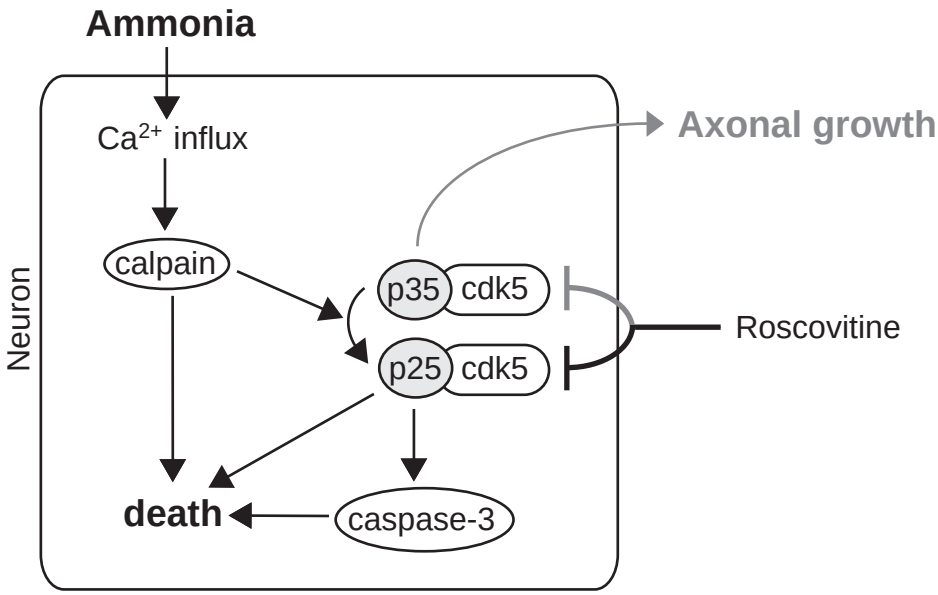

Cagnon & Braissant,
Figure 8

Legend for supplementary material

Supplementary figure 1. Impairment of axonal growth by ammonium exposure. **A**: Time course of axonal growth in brain cell aggregate control cultures between DIV 8 and 13. Axons are revealed at DIV 8, 11 and 13 by immunohistochemistry against phosphorylated NFM. **B**: Ammonium exposure impairs axonal growth, but does not induce axonal degeneration. Axons are revealed by immunohistochemistry against phosphorylated NFM, in control cultures or in cultures exposed to 5 mM NH_4Cl. All cultures harvested at DIV 13. Exposure to NH_4Cl: DIV 5-8, 5-11, 5-13, 8-11, 8-13 or 11-13. Scale bar = 50 µm.

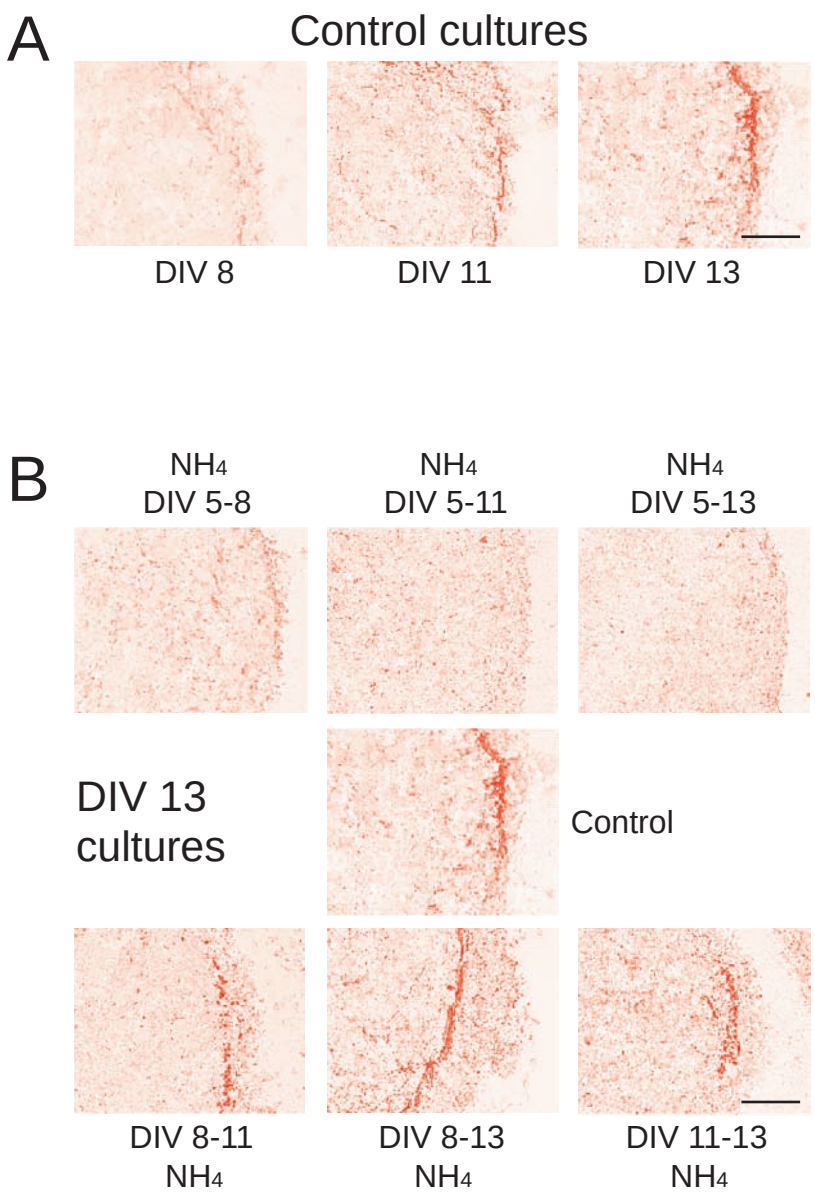

Cagnon & Braissant,
Supplementary Figure 1